Antisymmetric contribution to the planar Hall effect of Fe₃Si films grown on GaAs(113)*A* substrates

P. K. Muduli,* K.-J. Friedland, J. Herfort, H.-P. Schönherr, and K. H. Ploog

Paul-Drude-Institut für Festkörperelektronik, Hausvogteiplatz 5-7, D-10117 Berlin, Germany

The planar Hall effect (PHE) in ferromagnets is believed to result from the anisotropic magnetoresistance (AMR) and hence does not change the sign by reversing the direction of the applied in-plane magnetic field. Our studies of the ferromagnetic Heusler alloy Fe₃Si films grown on low-symmetric GaAs(113)A substrates however show a change in the sign of the PHE by reversing the direction of the applied field, indicating the existence of an additional antisymmetric component superimposed with the usual symmetric AMR term. This antisymmetric component shows a maximum along the major in-plane $\langle 33\bar{2} \rangle$ axes and vanishes along the other major in-plane $\langle \bar{1}10 \rangle$ axes. A phenomenological model based on the symmetry of the crystal provides a good explanation of the observed antisymmetric contribution to the PHE. The model shows that this component arises from the antisymmetric part of the magnetoresistivity tensor and is basically a second order Hall effect. It is shown that the observed effect can be ascribed to the Umkehr effect, which refers to the coexistence of even and odd terms in the component of magnetoresistivity tensor. A sign reversal of this antisymmetric component is also found for a Si content above 21 at. % and at temperatures below a certain critical temperature which increases with increasing Si content.

PACS number(s): 75.47.−m, 73.50.Jt, 73.43.Qt, 72.15.Gd

I. INTRODUCTION

Ferromagnet-semiconductor hybrid structures (FM/SC) have received significant attention for their possible application in spintronics.[1–3] Most of the previous studies of FM/SC were concentrated on low-index film orientation. Much less work has been devoted to study ferromagnetic films on high-index semiconductor substrates. In fact, obtaining a stable high-index surface of a ferromagnet in general is rather difficult. For instance, Fe films deposited on Cu(113) did not maintain the same orientational relationship with the substrate, which led to a highly strained and distorted bcc Fe arrangement with (112) orientation.[4] On the other hand, the thermal stability and ordering of such surfaces with reduced symmetry and coordination number offer the opportunities to manipulate the magnetic properties in FM/SC.[5] In a previous work,[6] we have reported on the successful growth of the Heusler alloy Fe₃Si on GaAs(113)A substrates. Fe₃Si has the cubic D0₃ crystal structure with a lattice constant very close to GaAs. This fact allows us to stabilize the [113] orientation of the Fe₃Si films on GaAs(113)A with structural properties comparable to those of Fe₃Si films on GaAs(001).[7] In this paper we will show that the magnetotransport properties, especially the planar Hall effect of these films are significantly affected by the reduced symmetry of the [113] orientation.

The so-called planar Hall effect (PHE) refers to the transverse voltage developed perpendicular to the current for a magnetic field applied in the film plane. It is believed to originate from a purely anisotropic magnetoresistance (AMR) effect[8] and depends on the angle between the magnetization and the direction of the sensing current. Suppose that a saturating external magnetic field, applied in the plane of the film, varies so that the angle θ_{M} of the magnetization **M** varies, then the resistivities ρ_{xx} and ρ_{xy} measured parallel and perpendicular to the current **J** for a single domain and polycrystalline film are given by[9,10]

$$\rho_{xx} = \rho_\perp + (\rho_\parallel - \rho_\perp)\cos^2\theta_{\mathrm{M}}, \qquad (1)$$

$$\rho_{xy} = \frac{1}{2}(\rho_\parallel - \rho_\perp)\sin 2\theta_{\mathrm{M}}, \qquad (2)$$

where $\rho_\perp$ and $\rho_\parallel$ are the resitivities at $\mathbf{J} \perp \mathbf{M}$, and $\mathbf{J} \parallel \mathbf{M}$, respectively. Equations (1) and (2) are conventionally used to describe the AMR and PHE, respectively. According to Eq. (2) we have $\rho_{xy}(H > +H_{\mathrm{sat}}) = \rho_{xy}(H < -H_{\mathrm{sat}})$, where H is the applied magnetic field and H_{sat} denotes the in-plane saturation field. This is understood from the fact that both AMR and PHE are believed to arise from the symmetric part of the magnetoresistivity tensor, which does not change sign when the direction of the magnetic field is reversed.[9] In this paper we will show that for single crystalline Fe₃Si films grown on low-symmetric GaAs(113)A substrates, Eq. (2) for the PHE is not strictly followed. In contrast, the PHE shows a combination of even (symmetric) and odd (antisymmetric) terms when a saturating magnetic field is applied in any direction other than the symmetric $\langle \bar{1}10 \rangle$ axes, indicating an observation of Umkehr effect.[11] The situation is similar to our previous experiments of Fe on GaAs(113)A substrates,[12,13] where we had reported an experimental observation of the effect. In this paper, we will develop a phenomenological model by taking into account the symmetry of the crystal to explain this effect. We will show how the observed antisymmetric component arises from a second order term of the antisymmetric part of the magnetorestivity tensor, as a result of the lower symmetry of the [113] orientation. The dependence of this antisymmetric component on the Si content of the Fe₃Si films and the measurement temperature will also be discussed. Possible reasons for the change in sign of this
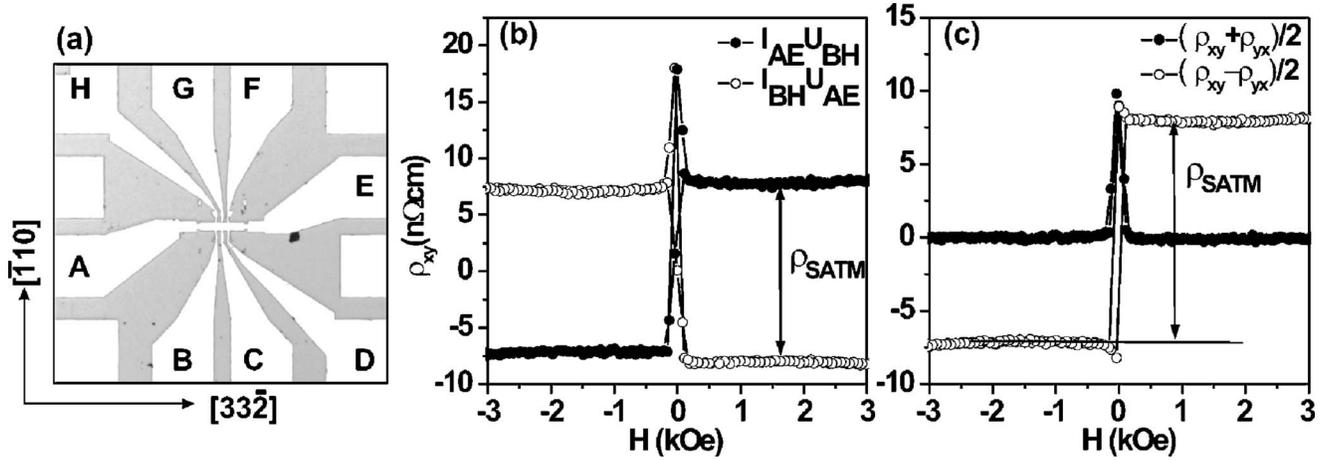
FIG. 1. (a) Optical microscopy image of the Hall bar structure employed for the magnetotransport studies. The contacts are labeled and the crystallographic directions of the (113) plane are shown. (b) Planar Hall effect response from $Fe_{3+x}Si_{1-x}$ films grown on GaAs(113)A at 300 K for a sample with $x=0.07$ and magnetic field applied along $[33\bar{2}]$. (c) Separation of the symmetric and antisymmetric contribution of PHE.

antisymmetric component with composition and temperature will also be discussed.

II. EXPERIMENT

$Fe_{3+x}Si_{1-x}$ films with thicknesses in the range of 35–50 nm were grown on well-ordered As-rich GaAs(113)A templates by molecular-beam epitaxy. Here x describes the deviation from the exact stoichiometry. The details of the growth can be found elsewhere.[6] It is important to note that the [113] orientation of $Fe_{3+x}Si_{1-x}$ has been stabilized on GaAs(113)A, which is in fact a result of the rather small lattice mismatch between Fe_3Si and GaAs. The Si content was carefully varied in the range of 15–26.6 at. % Si, i.e., $0.4 > x > -0.06$ which lies within the phase boundary of the stable Fe_3Si phase covering a range from 9 to 26.6 at. %Si.[14,15]

For the magnetotransport measurements Hall bar structures as shown in Fig. 1(a) were prepared by standard lithography techniques. The Hall bars were aligned along the $[33\bar{2}]$ direction by a combination of photolithography and ion-beam sputtering. A perfect alignment of the Hall bar structures ensures a homogenous current flow. Both AMR (ρ_{xx}) and PHE (ρ_{xy}) were measured simultaneously with a current of 3 mA along the Hall bar. A programmable stepper motor was used for the rotation of the sample in the magnetic field. Two different kinds of measurements were performed. First, we studied the angular dependence of the PHE response when a fixed in-plane magnetic field was applied. Second, the in-plane field orientation was kept fixed along a specific direction with respect to the longitudinal axis of the Hall bars, while the field magnitude was swept linearly between ± 3 kOe. As the low transverse Hall resistivity, ρ_{xy} is smaller than the longitudinal resistivity, ρ_{xx}, some crossover from ρ_{xx} to ρ_{xy} may appear. In this case, we have corrected ρ_{xy} by $\rho_{xy}^{\text{corr}}(H,\theta_H) = \rho_{xy}(H,\theta_H) - \gamma \rho_{xx}(H,\theta_H)$, where the factor γ was kept constant for a particular contact configuration.

III. RESULTS AND DISCUSSION

A. Experimental results

1. Antisymmetric component in PHE

In Fig. 1, we show the room temperature (300 K) PHE response from a nearly stoichiometric $Fe_{3+x}Si_{1-x}$ sample with $x=0.07$. An optical microscopy image of the Hall bar structure employed is shown in Fig. 1(a) with the contacts labeled as A, B,….,H in a counterclockwise sense. The PHE response is depicted in Fig. 1(b) for two cases with the current along AE and BH, which correspond to the $[33\bar{2}]$ and $[\bar{1}10]$ directions, respectively. The magnetic field was kept fixed along the $[33\bar{2}]$ direction. The planar Hall voltage was measured along the contacts BH and AE for the current along AE and BH, respectively. We denote the two cases $I_{AE}U_{BH}$ and $I_{BH}U_{AE}$ by ρ_{xy} and ρ_{yx}, respectively. Here, the positive x axis is taken along the $[33\bar{2}]$ direction. As can be seen, the PHE is completely saturated at a rather low field of less than 0.2 kOe (Ref. 16) but the PHE shows a sign change with reversal of the magnetic field direction, irrespective of the current direction. This was never observed in Fe and $Fe_{3+x}Si_{1-x}$ films grown on GaAs(001) substrates[13,17] and is completely unexpected from Eq. (2), which predicts only a symmetric contribution.[8,9] Also ρ_{xy} and ρ_{yx} have opposite signs just like the conventional Hall effect. This implies the presence of an antisymmetric component in PHE for the $Fe_{3+x}Si_{1-x}$ films on GaAs(113)A. In fact, the symmetric and the antisymmetric contribution can be separated by adding and subtracting the signals ρ_{xy} and ρ_{yx}, which is shown in Fig. 1(c). We clearly have an additional antisymmetric contribution to the PHE superimposed to the usual symmetric contribution of Eq. (2). Since the sample is completely saturated, we can rule out any contribution of domains to this effect. We define the difference, $\rho_{xy}(H > +H_{sat}) - \rho_{xy}(H < -H_{sat})$ as a saturated antisymmetric transverse resistivity ρ_{SATM}, which is a measure of the antisymmetric component. When the sample is rotated slightly out-of-plane, the contribution from the anomalous

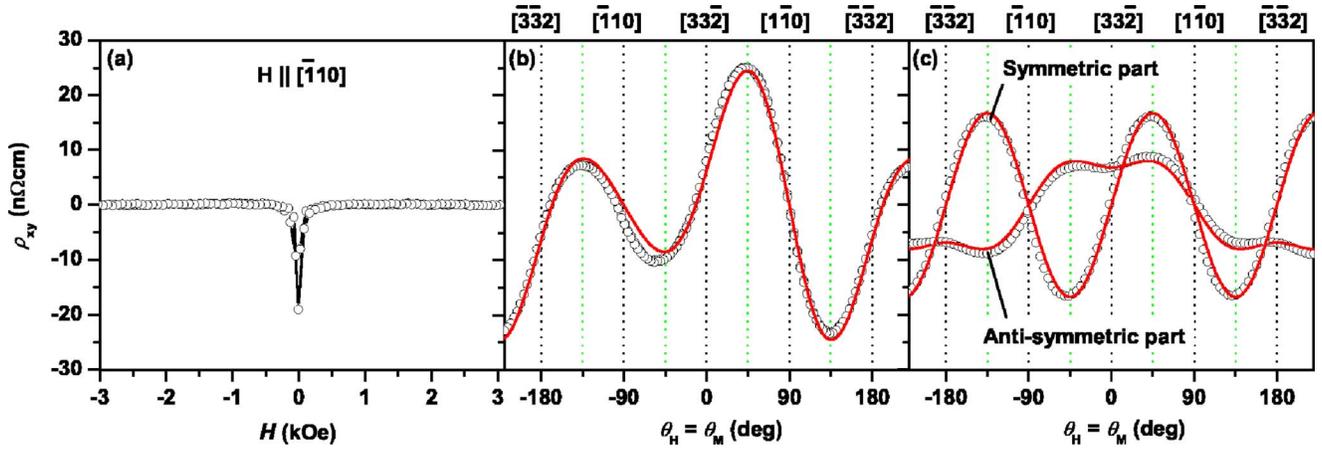FIG. 2. (Color online) (a) Planar Hall effect response from the $Fe_{3+x}Si_{1-x}$ ($x=0.07$) film grown on GaAs(113)A with magnetic field applied in-plane along $[\bar{1}10]$ at 300 K showing the vanishing antisymmetric component. (b) Angular dependence of ρ_{xy} at 300 K with a saturating in-plane magnetic field so that $\theta_H = \theta_M$. Open circles represent experimental data and solid line (in red color) is a fit using Eq. (3) (see text). (b) Separation of the symmetric and antisymmetric part of the PHE. Open circles represent experimental data and solid lines (in red color) are fitted curves using a $\sin 2\theta_M$ behavior for symmetric part and $\rho_{SATM}^0 \cos \theta_M + \rho_{SATM}^1 \cos^3 \theta_M$ type behavior for antisymmetric part. The major in-plane crystallographic directions for the (113) plane are also shown with 0° along $[33\bar{2}]$.

Hall effect (AHE) starts to appear as a slope in the high field region which is similar to that observed in Fe films on GaAs(113)A substrates.[12] But ρ_{SATM} does not vanish when a magnetic field is applied slightly out-of-plane in different directions. Since we are dealing with an antisymmetric contribution, the direction of the applied field relative to the current and the orientation of transverse resistivity determine the sign of ρ_{SATM}. To define the sign of ρ_{SATM}, from now on we will stick to the convention that the current is applied along AE and the PHE is measured along BH. For this configuration we found a positive sign of ρ_{SATM} (in the sample with $x=0.07$) at 300 K with a magnetic field applied along the $[33\bar{2}]$ direction. Of course the sign of ρ_{xy} changes when the direction of the field is reversed by 180°, i.e., toward $[\bar{3}\bar{3}2]$. But, fortunately these two directions can be identified unambiguously from x-ray diffraction (XRD) by measuring an asymmetric reflection such as (004). We can thus keep the field direction fixed along $[33\bar{2}]$ which has been confirmed for all samples by XRD. The positive direction of the magnetic field was defined in such a way that the Hall voltage in this configuration is negative for a n-type semiconductor sample.

When the magnetic field is aligned along the $\langle \bar{1}10 \rangle$ axes, the antisymmetric component vanishes ($\rho_{SATM}=0$) as shown in Fig. 2(a). Since this is a common in-plane axis with the (001) plane, ρ_{SATM} must be related to the symmetry of the [113] orientation. The dependence of ρ_{xy} on the field orientation angle θ_H (defined with respect to the $[33\bar{2}]$ direction) can be more clearly seen in Fig. 2(b), which shows the angular dependence of PHE measured at 300 K with a fixed positive saturating magnetic field ($H=+1$ kOe). The field orientation angle θ_H is varied from $-220°$ to $+220°$ in the plane of the sample. The high field ensures a complete saturation of the sample so that $\theta_H = \theta_M$. The angular dependence is completely reversible and does not follow the $\sin 2\theta_H$ de-

pendence of Eq. (2). A separation of the symmetric and antisymmetric component can be achieved by taking the sum and difference of the angular dependence of the PHE for positive and negative fields above saturation. The result is shown in Fig. 2(c). The symmetric part follows the well-known $\sin 2\theta_H$ dependence of Eq. (2). The antisymmetric part, on the other hand, can be fitted by an equation of the form $\rho_{SATM}^0 \cos \theta_H + \rho_{SATM}^1 \cos^3 \theta_H$, shown by the solid line, where ρ_{SATM}^0 and ρ_{SATM}^1 are arbitrary constants to be interpreted. Using this functional form, the PHE response from $Fe_{3+x}Si_{1-x}(113)$ films can be modified to

$$\rho_{xy} = \rho_s^{PHE} \sin 2\theta_H + \rho_{SATM}^0 \cos \theta_H + \rho_{SATM}^1 \cos^3 \theta_H, \quad (3)$$

where we have introduced a constant ρ_s^{PHE} to take into account the experimental observation that $(\rho_\parallel - \rho_\perp)$ derived from the PHE response [by using Eq. (2)] is smaller than that derived from the ρ_{xx} response. In this particular sample, both quantities differ by one order of magnitude (see Fig. 5). Here $\theta_H = 0°$ is defined with respect to the current direction, which is along the $[33\bar{2}]$ direction. Using this modified equation for the PHE, we fit the angular dependence of Figs. 2(b) and 2(c) which are shown as solid lines. The best fitting is obtained for $\rho_s^{PHE}=16.5$ nΩ cm, $\rho_{SATM}^0=16$ nΩ cm, and $\rho_{SATM}^1 =-10$ nΩ cm.

2. Composition and temperature dependence of the antisymmetric component in PHE

In Fig. 3 we show the field and angular dependence of ρ_{xy} for the same $Fe_{3+x}Si_{1-x}(113)$ film ($x=0.07$) at 77 K. Figure 3(a) shows the field dependence of ρ_{xy} with magnetic field applied parallel to $[33\bar{2}]$. As can be seen, the sign of the antisymmetric component is reversed, i.e, ρ_{SATM} is negative in contrast to the positive value of ρ_{SATM} at 300 K [see Fig. 1(a) for the configuration $I_{AE}U_{BH}$]. Figures 3(b) and 3(c) show the corresponding dependencies of ρ_{xy} on the field ori-
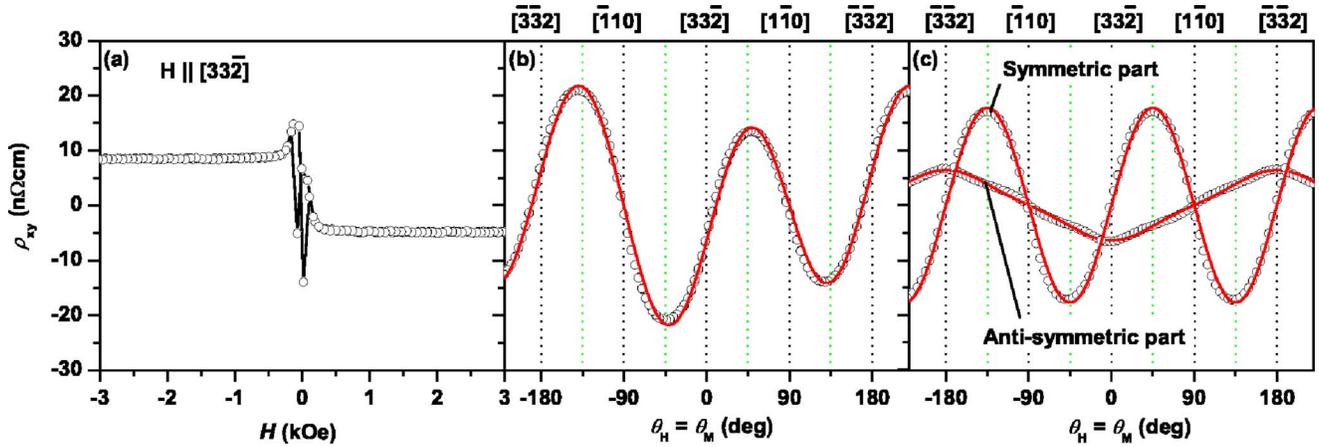
FIG. 3. (Color online) (a) Planar Hall effect response from $Fe_{3+x}Si_{1-x}(113)$ ($x=0.07$) film at 77 K with magnetic field applied in-plane along $[33\bar{2}]$. (b) Corresponding angular dependence of ρ_{xy} at 77 K with a saturating in-plane magnetic field so that $\theta_H = \theta_M$. (c) Separation of the symmetric and antisymmetric part of the PHE. Open circles represent experimental data and solid lines (in red color) are fitted curves as explained in Fig. 2.

entation angle θ_H at a saturating field ($\theta_H = \theta_M$). The open circles represent experimental data and the solid lines are the fitted curves using Eq. (3) similar to Figs. 3(b) and 3(c). The best fitting is obtained for $\rho_s^{PHE}=17.8$ nΩ cm, $\rho_{SATM}^0=-4.4$ nΩ cm, and $\rho_{SATM}^1=-2$ nΩ cm. The change in sign of ρ_{SATM} is clearly seen. To study the temperature and composition dependence of the antisymmetric component in more detail, we have measured the difference: $\rho_{SATM}=\rho_{xy}(H>+H_{sat})-\rho_{xy}(H<-H_{sat})$ for a series of samples with x varying from +0.39 to −0.04 and temperatures varying from 300 to 4 K. The saturating magnetic field was applied along $[33\bar{2}]$, so that $\rho_{SATM}=2(\rho_{SATM}^0+\rho_{SATM}^1)$ [see Eq. (3)]. The results are summarized in Fig. 4(a), which shows several important results. First, ρ_{SATM} decreases with decreasing x and temperature (except the sample with $x=-0.04$). Second, ρ_{SATM} changes sign below a certain critical temperature which increases with decreasing x (increase of Si content). Interestingly, the sign of ρ_{SATM} for samples very close to stoichiometry ($x\sim0$) is negative at RT, which is the same as in Fe films grown on GaAs(113)A substrates.[13] However, for Fe films on GaAs(113)A no change in sign of ρ_{SATM} has been observed in the measurement temperature range of 4 to 300 K.

3. Anisotropic magnetoresistance

Before concluding this section of experimental results, we will show that the AMR response from these $Fe_{3+x}Si_{1-x}(113)$ samples can be well-described by Eq. (1). The results of AMR (ρ_{xx}) measurements are summarized in Fig. 5 for the sample with $x=0.07$. Clearly, ρ_{xx} is a symmetric function of the applied field direction [see Fig. 5(a)] and the angular dependence of ρ_{xx} for a saturating field shows a perfect $\cos^2\theta_M$ dependence [see Figs. 5(b) and 5(c)]. Surprisingly, the ρ_{xx} amplitude, ($\rho_\parallel-\rho_\perp$), which is the difference of ρ_{xx} for 0° and 90°, is negative but is similar to our previous findings on $Fe_{3+x}Si_{1-x}$ films on GaAs(001).[17] For this sample with $x=0.07$, a clear change in sign of ρ_{SATM} was observed at about 150 K [see Fig. 4(a)], however, no change in sign of

($\rho_\parallel-\rho_\perp$) is observed even at 77 K [see Fig. 5(c)]. This implies that the change in sign of ρ_{SATM} is uncorrelated to any AMR based mechanism such as the different electron mean free path as suggested by Granberg *et al.*[18] in AMR studies of Fe films. The negative value of ($\rho_\parallel-\rho_\perp$), which is just opposite to that of the Fe, indicates a different spin-dependent scattering mechanism.[9]

From our superconducting quantum interference device (SQUID) magnetometry studies, the magnetic anisotropy of these [113] oriented samples are well known to exhibit a dominant in-plane fourfold magnetic anisotropy, with the easy axes along the in-plane $\langle\bar{3}01\rangle$ axes.[6] The saturation magnetization M_s of these Fe_3Si films as measured by
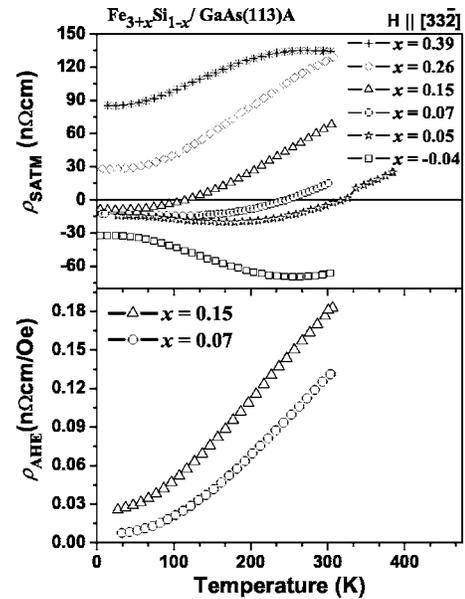

FIG. 4. (a) Temperature and composition dependence of the $\rho_{SATM}=\rho_{xy}(H>+H_{sat})-\rho_{xy}(H<-H_{sat})$ measured with a saturating field applied near to the $[33\bar{2}]$ direction. (b) Temperature dependence of ρ_{AHE} for two typical samples with $x=0.07$ and 0.15.
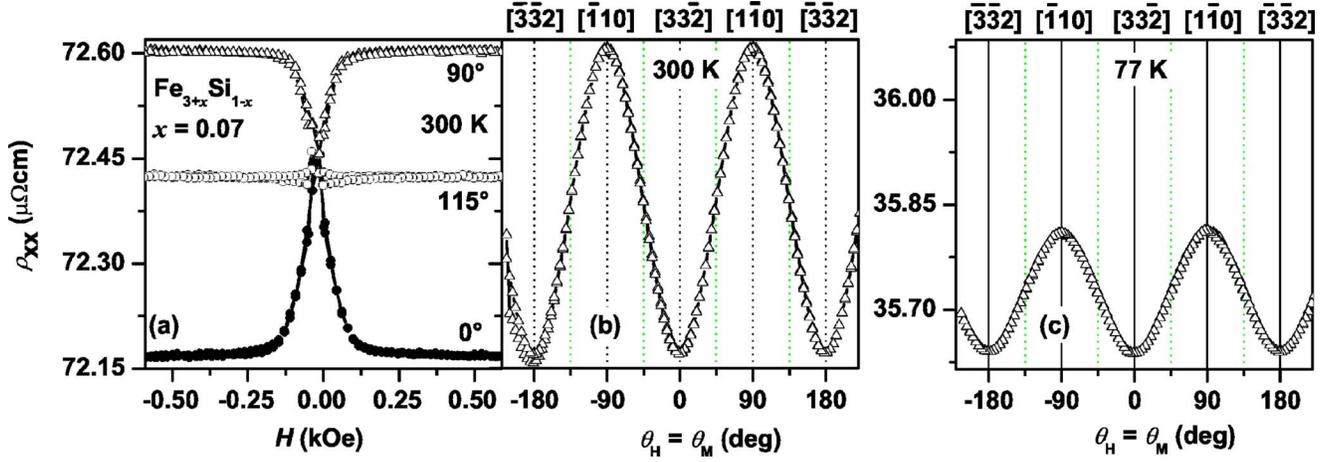
FIG. 5. (Color online) (a) Field dependence of the AMR (ρ_{xx}) from the $Fe_{3+x}Si_{1-x}(113)$ film with $x=0.07$ at 300 K for different in-plane orientations. The open circles represent the easy axis of magnetization, for which the AMR signal does not change. Angular dependence of ρ_{xx} at a fixed saturating field of $H=1$ kOe obtained at (b) 300 K and (c) 77 K. For comparison, the amplitude of AMR is kept fixed for the three figures.

SQUID magnetometry is between 500 and 1450 emu/cm³ at 300 K, where M_s decreases with increasing Si content.[6] This corresponds to a demagnetization field ($=4\pi M_s$) of about 6.2–18.2 kOe which is much larger than the measured low in-plane saturation field ($\simeq 2K_1/M_s$) of <200 Oe. The large demagnetization energy does not allow the moment to rotate out-of-plane. Hence, in all the samples reported here, the magnetization lies in-plane. In fact, the in-plane four-fold magnetic anisotropy is a consequence of the magnetocrystalline anisotropy similar to that of Fe films on GaAs(113)A substrates.[19] Because of the high Curie temperature of these samples, the temperature dependence of the magnetic properties is weak and did not show any significant differences. The magnetic anisotropy is also obvious from the field dependent behavior of ρ_{xx} in Fig. 5(a). However, a detailed discussion of the magnetic anisotropy is not relevant in the present discussion, since our main focus here is about a true saturating property.

B. Phenomenological model

In this section we will present a phenomenological model,[9,20] based on the symmetry of the crystal to understand the origin of the antisymmetric component in the PHE of single crystalline $Fe_{3+x}Si_{1-x}$ films grown on low-symmetric GaAs(113)A substrates. When a saturating field **H** with components $H_i=H\alpha_i$, is applied to a crystal, the relationship between the electric field **E** and current density **J** is defined through the relation

$$E_i = \rho_{ij}(\alpha)J_j, \quad (4)$$

where, $\rho_{ij}(\alpha)$ is the second rank magnetoresistivity tensor and E_i and J_j are components of the electric field **E** and current density **J**, respectively. The tensor $\rho_{ij}(\alpha)$ depends on the direction cosines, α_i, of the magnetization vector and hence can be expressed as a series expansion in ascending powers of the α_i[9,20]

$$\rho_{ij}(\alpha) = a_{ij} + a_{kij}\alpha_k + a_{klij}\alpha_k\alpha_l + a_{klmij}\alpha_k\alpha_l\alpha_m + \cdots, \quad (5)$$

where the Einstein summation convention is understood. The tensors with elements $a_{ij}, a_{kij}, a_{klij}\cdots$, simplify due to the crystal symmetry.[20] The tensor $\rho_{ij}(\alpha)$ being of second rank can be divided into its symmetrical and antisymmetrical parts,

$$\rho_{ij}^s(\alpha) = \frac{1}{2}[\rho_{ij}(\alpha) + \rho_{ji}(\alpha)] \quad (6)$$

and

$$\rho_{ij}^a(\alpha) = \frac{1}{2}[\rho_{ij}(\alpha) - \rho_{ji}(\alpha)]. \quad (7)$$

Onsager's theorem[20] applied to a magnetically saturated crystal gives

$$\rho_{ij}(\alpha) = \rho_{ji}(-\alpha), \quad (8)$$

so that that ρ_{ij}^s is an even function of the α_i and ρ_{ij}^a is an odd function of the α_i.

For both contributions, we have the power series

$$\rho_{ij}^s(\alpha) = a_{ij} + a_{klij}\alpha_k\alpha_l + \cdots \quad (9)$$

and

$$\rho_{ij}^a(\alpha) = a_{kij}\alpha_k + a_{klmij}\alpha_k\alpha_l\alpha_m + \cdots. \quad (10)$$

Traditionally, if one considers the leading terms (up to second order in α_i) in above equations and neglect the higher order terms, the associated electric fields $\mathbf{E}_s$ and $\mathbf{E}_a$ represent the generalized magnetoresistance and Hall effects, respectively.[9,20,21] With this consideration, PHE for which the magnetic field is applied in-plane, should arise from ρ_{ij}^s and should also be an even function of the applied field direction. However, in our PHE experiments on the $Fe_3Si(113)$ films [also on Fe(113) films], we see an addi-

tional component, which is an odd function of the magnetic field direction. Consequently, this component must involve an antisymmetrical part ρ_{ij}^a.

Before proceeding further we will need to derive all the components of the magnetoresistivity tensor ρ_{ij} for the classical crystal class **m3m**, to which both Fe$_3$Si (F**m3m**) and Fe (I**m3m**) belong. The D0$_3$ crystal structure of Fe$_3$Si belongs to the space group F**m3m**. Details can be found in Appendix A. Let us first consider the simple case of an (001) oriented thin-film, with current $J=(J_1,0,0)$ along the [100] direction. We assume that the magnetization **M** lies in the (001) plane, making an angle θ_M to the current. In this case the measured Hall voltage is given by

$$E_2 = \rho_{21}J_1, \qquad (11)$$

where the indexes 1, 2, and 3 refer to the x, y, and z axes, respectively. The α_is are given by $\alpha_1 = \cos\theta_M$, $\alpha_2 = \sin\theta_M$, and $\alpha_3 = 0$. The planar Hall resistivity can be found by substituting the α_is in Eq. (A2)

$$\rho_{21} = \frac{C_4}{2}\sin 2\theta_M, \qquad (12)$$

which is similar to the well-known $\sin 2\theta_M$ relation of Eq. (2). However, the prefactor of $\sin 2\theta_M$ in the above equation, i.e., C_4 is no longer equal to the AMR amplitude, $\rho_\parallel - \rho_\perp$ for the single crystalline samples.[22] It may be mentioned that the prefactor $\rho_\parallel - \rho_\perp$ in Eq. (2) for the polycrystalline films result from the averaging over a large number of randomly oriented crystallites.[8,22] Nevertheless, the coefficient C_4 as introduced in Appendix A is a coefficient from the symmetric part of the tensor ρ_{ij}^s, and hence traditionally PHE is attributed to an AMR effect.[8,21] Now we consider the case of the low-symmetric [113] oriented films. The measurements were performed with a current in the [33$\bar{2}$] direction and the Hall voltage was measured along the [$\bar{1}$10] direction. Thus, to find the measured planar Hall resistivity, we must perform a coordinate transformation[20,23] of ρ_{21}. This transformation is performed in Appendix B. The final equation for the measured planar Hall resistivity in (113) films is given in Eq. (B4) of Appendix B. If we consider terms up to third order of α_i, we can write the measured Hall resistivity for the (113) films in the following way:

$$\rho_{21}^{(113)} = \frac{(9C_1 + 2C_4)}{22}\sin 2\theta_M + \frac{9(a_{12223} - a_{11123})}{11\sqrt{2}}\cos\theta_M$$
$$- \frac{42\sqrt{2}(a_{12223} - a_{11123})}{121}\cos^3\theta_M, \qquad (13)$$

which agrees with Eq. (3) for $\rho_s^{PHE} = (9C_1 + 2C_4)/22$, $\rho_{SATM}^0 = 9(a_{12223} - a_{11123})/(11\sqrt{2})$, and $\rho_{SATM}^1 = -42\sqrt{2}(a_{12223} - a_{11123})/121$. The coefficient C_1 is also introduced in Appendix A. Here, for the symmetric part, we have considered terms up to the second order of α_i as described in the first term with the well-known $\sin 2\theta_M$ dependence. However, as the most exciting result of this calculation, there are two additional terms which arise from the antisymmetric part of the tensor ρ_{ij}^a. *These are third-order contributions of α_i and*

arise from the lower symmetry of the (113) plane, where the magnetization **M** *rotates due to the large demagnetization energy of the* Fe$_3$Si *films*. It is easy to show that these additional antisymmetric terms vanish for magnetic fields applied along the $\langle\bar{1}10\rangle$ axes ($\theta_M = 90°$) and change sign with the change in the direction of the applied magnetic field along all other in-plane directions. Hence, this equation provides a perfect explanation of the antisymmetric contribution observed in the PHE (Sec. III A 1). Both ρ_{SATM}^0 and ρ_{SATM}^1 contain the difference $(a_{12223} - a_{11123})$, which could be of either sign from the viewpoint of symmetry. Thus $\rho_{SATM} = 2(\rho_{SATM}^0 + \rho_{SATM}^1)$ can be both positive and negative in agreement with the experimental results (Sec. III A 2). It should be mentioned that this additional antisymmetric component could not be obtained on the high-symmetric (001) plane in agreement with experiments on [001] oriented ferromagnetic thin films.[13,17] The appearance of third-order contributions of α_i is not surprising, since to describe the magnetoresistivity anisotropy effects terms up to a fourth-order contribution of α_i has been shown to be necessary.[24,25] These third-order terms in α_i can be termed as a second order Hall effect [see Eq. (10)]. The fourth-order terms contribute additional $\sin 2\theta_M$ and $\sin 4\theta_M$ terms which are symmetric and are neglected for simplicity. This is justified, since to describe the experimental data, terms up to third orders, as considered in the above Eq. (13) are found sufficient.

The coexistence of even and odd terms in the component of magnetoresistivity tensor in the above Eq. (13) has been called the Umkehr effect[11] in literature. This effect was discussed theoretically in 1975 by Akgöz and Saunders[26] based on the symmetry restrictions on the form of galvanomagnetic/thermomagnetic tensors. Experimentally, the Umkehr effect was observed in thermomagnetic effects[11,26] and magnetotransport[27] measurements in Bismuth. As pointed out by Akgöz and Saunders,[26] the effect is not restricted to the trigonal crystal structure of Antimony and Bismuth and the Umkehr effect can also be observed in cubic crystals depending on the measurement geometry as considered in the present case.

It is also possible to show within this phenomenological approach that the AMR Eq. (1) is valid even for this low-symmetric orientation, in agreement with the experimental observations. The longitudinal resistivity, $\rho_{xx}^{(113)}$ can be derived in the same manner

$$\rho_{xx}^{(113)} = \rho_{11}^{(113)} \approx C_0 + \frac{9}{22}(C_1 - C_4) + \frac{126C_4 - 5C_1}{121}\cos^2\theta_M, \qquad (14)$$

which reproduces Eq. (1) for $\rho_\perp = C_0 + 9(C_1 - C_4)/22$ and $(\rho_\parallel - \rho_\perp) = (126C_4 - 5C_1)/121$. This equation also provides a good explanation for the experimental observation $\rho_s^{PHE} \neq (\rho_\parallel - \rho_\perp)$, which in fact is a result of the single crystalline nature of the sample.

Now we will discuss the sign change of ρ_{SATM} with composition and temperature. For Fe$_3$Si films on GaAs(001) substrates we previously observed a sign change in the PHE due to the ordering toward the stoichiometric Fe$_3$Si

composition.[17] However, in that case the PHE was a symmetric function of the applied field direction. But ρ_{SATM} is an antisymmetric contribution (in fact a second-order Hall effect) and hence a similar origin, like the AHE is most likely responsible. In fact, the change in sign of the AHE in binary alloys with composition and temperature is rather well known.[28–32] The anomalous Hall resistivity ρ_{AHE} for a saturating magnetic field and for the (113) symmetry also involves the tensor elements a_{12223} and a_{11123}

$$\rho_{AHE}^{(113)} = \frac{1}{121}(121a_{123} + 83a_{11123} + 38a_{12223}). \quad (15)$$

This can be found easily by using Eqs. (11) and (A2) for a saturating magnetic field applied along the normal [113]. In this equation, the first term containing the usual tensor element a_{123}, represents a first-order contribution of α_i, whereas the other two terms are third-order contributions just like in the PHE. The presence of the same tensor elements a_{11123} and a_{12223} in PHE and AHE may imply a similar physical origin of ρ_{SATM} and ρ_{AHE}. To see whether ρ_{AHE} also changes sign with temperature, we measured AHE for samples with $x=0.07$ and $x=0.15$, in which a clear change in sign of ρ_{SATM} was observed at about 150 and 250 K, respectively. In Fig. 4(b), we show the behavior of ρ_{AHE} with temperature for these two samples. As can be seen, no change in sign of ρ_{AHE} is observed for both samples. However, this may be understood from the fact that ρ_{SATM} is a higher-order contribution, and in AHE this contribution is not the most significant ones. [See Eqs. (13) and (15).]

At the end, we will discuss the possible origin of the observed sign change of the antisymmetric component. First we will like to mention yet another observation from the results of high-resolution x-ray diffraction (HRXRD) measurements which was performed using a PANalytical X'Pert diffractometer. In HRXRD a study of the crystal or atomic ordering of these Fe_3Si films was performed by analyzing different superlattice reflections similar to our recent studies of long-range ordering of Fe_3Si films on GaAs(001).[33] For the $D0_3$ crystal structure of Fe_3Si, Bragg reflections are produced by either all odd or all even Miller indices (h,k,l). The reflections for which h,k,l are all even with $\frac{1}{2}(h+k+l)=2n$, n being an integer, are fundamental reflections and are unaffected by the state of ordering. The reflections for which h,k,l are all even with $\frac{1}{2}(h+k+l)=2n+1$ is sensitive to a $(A,C) \rightarrow D$ disorder whereas the reflections for which all the h,k,l odd are sensitive to both $B \rightarrow D$ and $(A,C) \rightarrow D$ disorder, where the notations A,C, and D refer to different sublattice of Fe_3Si as described in the literature.[34–36] The sublattices A,B, and C are occupied by Fe atoms whereas the sublattice D is occupied by Si atoms. The relative intensity of these two classes of reflections depends on the state of ordering, but for a prefect ordered lattice the intensities should be equal.[33,36,37] For example, the (002) reflection and the (113) reflections should have the same intensity for a perfectly ordered Fe_3Si lattice. We found an increase in the intensity of the (002) reflection with increasing Si content. The superlattice and symmetric (113) reflection with h,k,l being all odd was detectable only for samples with a Si content of 26 at. % ($x=-0.04$). Hence, a good long-range atomic order is found in the nearly stoichiometric as-grown films which also establish the formation of a $D0_3$ crystal structure. As discussed before in the context of Fig. 4(a), the stoichiometric samples have a negative sign of ρ_{SATM} (for a magnetic field applied along $[33\bar{2}]$) at 300 K. Fe samples on GaAs(113)A also have a negative sign of ρ_{SATM} at 300 K. Since both Fe and Fe_3Si belong to the same crystal class, there seems to have some correlation between the two phenomena (the negative sign of the ρ_{SATM} and the improvement of atomic ordering). A microscopic theory of electron transport may provide further understanding of this possible correlation. In principle, when all the restrictions imposed by the band structure symmetry are included in such a calculation, the form obtained for PHE should be identical to that found from the phenomenological model.

IV. CONCLUSION

We have performed an extensive study of the magnetotransport properties of Fe_3Si films grown on GaAs(113)A substrates by molecular-beam epitaxy. The PHE of these films show an additional antisymmetric contribution, which arises from the lower symmetry of the [113] orientation and large demagnetization energy of the Fe_3Si films. A phenomenological model developed to understand the observed experimental data provides good explanation of the antisymmetric component and shows that this additional component comes from the antisymmetric part of the magnetoresistivity tensor like for the conventional Hall effect. It is shown that the observed effect can be ascribed to the Umkehr effect, which refers to the coexistence of even and odd terms in the component of magnetoresistivity tensor. This additional antisymmetric component is found to change the sign by varying the Si content in $Fe_{3+x}Si_{1-x}$ films and the measurement temperature. In fact the sign reversal occurs for a Si content above 21 at. % and at temperatures above a certain critical temperature which increases with increasing Si content. The microscopic origin of this additional contribution is not yet understood.

APPENDIX A: DETERMINATION OF COMPLETE MAGNETORESISTIVITY TENSOR ELEMENTS FOR THE CRYSTAL CLASS M3M

In matrix notation the magnetoresitivity tensor ρ_{ij} can be written as

$$\rho = \begin{pmatrix} \rho_{11} & \rho_{12} & \rho_{13} \\ \rho_{21} & \rho_{22} & \rho_{23} \\ \rho_{31} & \rho_{32} & \rho_{33} \end{pmatrix}. \quad (A1)$$

The elements ρ_{ij} can be expressed in terms of the tensors $a_{ij}, a_{kij}, a_{klij}$, etc.. As already mentioned, the elements of these tensors simplify due to the crystal symmetry. For the crystal class **m3m**, the nonzero elements are tabulated by Birss.[20] Mcguire and Potter[9] derived the elements of the symmetric magnetoresistivity tensor ρ_{ij}^s through fifth order for the crystal class **m3m**. The antisymmetric magnetoresistivity tensor ρ_{ij}^a can be derived using the nonzero coefficients of the tensors $a_{ij}, a_{kij}, a_{klij}, \ldots$, etc. listed by Birss.[20] The resulting elements ρ_{ij} of Eq. (A1) can be written as follows

$$\rho_{11} = C_0 + C_1\alpha_1^2 + C_2\alpha_1^4 + C_3\alpha_2^2\alpha_3^2$$

$$\rho_{12} = C_4\alpha_1\alpha_2 + C_5\alpha_1\alpha_2\alpha_3^2 + (a_{123}\alpha_3 + a_{12223}\alpha_1^2\alpha_3$$
$$+ a_{12223}\alpha_2^2\alpha_3 + a_{11123}\alpha_3^3)$$

$$\rho_{13} = C_4\alpha_1\alpha_3 + C_5\alpha_1\alpha_3\alpha_2^2 - (a_{123}\alpha_2 + a_{12223}\alpha_1^2\alpha_2 + a_{11123}\alpha_2^3$$
$$+ a_{12223}\alpha_2\alpha_3^2)$$

$$\rho_{21} = C_4\alpha_1\alpha_2 + C_5\alpha_1\alpha_2\alpha_3^2 - (a_{123}\alpha_3 + a_{12223}\alpha_1^2\alpha_3$$
$$+ a_{12223}\alpha_2^2\alpha_3 + a_{11123}\alpha_3^3)$$

$$\rho_{22} = C_0 + C_1\alpha_2^2 + C_2\alpha_2^4 + C_3\alpha_3^2\alpha_1^2$$

$$\rho_{23} = C_4\alpha_2\alpha_3 + C_5\alpha_2\alpha_3\alpha_1^2 + (a_{123}\alpha_1 + a_{11123}\alpha_1^3 + a_{12223}\alpha_1\alpha_2^2$$
$$+ a_{12223}\alpha_1\alpha_3^2)$$

$$\rho_{31} = C_4\alpha_1\alpha_3 + C_5\alpha_1\alpha_3\alpha_2^2 + (a_{123}\alpha_2 + a_{12223}\alpha_1^2\alpha_2 + a_{11123}\alpha_2^3$$
$$+ a_{12223}\alpha_2\alpha_3^2)$$

$$\rho_{32} = C_4\alpha_2\alpha_3 + C_5\alpha_2\alpha_3\alpha_1^2 - (a_{123}\alpha_1 + a_{11123}\alpha_1^3 + a_{12223}\alpha_1\alpha_2^2$$
$$+ a_{12223}\alpha_1\alpha_3^2)$$

$$\rho_{33} = C_0 + C_1\alpha_3^2 + C_2\alpha_3^4 + C_3\alpha_1^2\alpha_2^2, \quad \text{(A2)}$$

where the C_0, C_1, C_2, C_3, etc. are short-hand notations of Mcguire and Potter[9] for the coefficients in the symmetric part of magnetoresistivity tensor ρ_{ij}^s given by the following equations:

$$C_0 = a_{11} + a_{1122} + a_{111122}$$

$$C_1 = a_{1111} - a_{1122} - 2a_{111122} + a_{112211}$$

$$C_2 = a_{111111} + a_{111122} - a_{112211}$$

$$C_3 = a_{112233} - 2a_{111122}$$

$$C_4 = a_{2323} + a_{111212}$$

$$C_5 = a_{112323} - a_{111212}. \quad \text{(A3)}$$

The factors in the brackets of Eq. (A2) arise from the antisymmetric part of the tensor ρ_{ij}^a. For the diagonal elements, the antisymmetric part is zero, whereas the off-diagonal elements satisfy the following relation:

$$\rho_{ij}^a = -\rho_{ji}^a, \quad \text{when i} \neq \text{j.} \quad \text{(A4)}$$

APPENDIX B: TRANSFORMATION INTO THE (113) SYSTEM

We use the following matrix l which transforms the (001) basis vector system to the basis vector system of (113):

$$l = \begin{pmatrix} \frac{3}{\sqrt{22}} & \frac{3}{\sqrt{22}} & -\sqrt{\frac{2}{11}} \\ -\frac{1}{\sqrt{2}} & \frac{1}{\sqrt{2}} & 0 \\ \frac{1}{\sqrt{11}} & \frac{1}{\sqrt{11}} & \frac{3}{\sqrt{11}} \end{pmatrix}. \quad \text{(B1)}$$

The elements of this matrix l_{ij} are determined by the relative orientation of the old and new sets of axes, e.g., $l_{12} = \cos \widehat{x_2 O x_1'}$, where Ox_2 and Ox_1' are the old y axis and the new x axis, respectively (see Birss[20] for details). In our case l_{12} presents the cosine of the angle between the [010] and the $[33\bar{2}]$ axis. According to the measurements, we choose the new x axis along $[33\bar{2}]$, y axis along $[\bar{1}10]$, and z axis along [113]. To find the measured planar Hall resistivity in the new co-ordinate system we need to use the transformation properties of a second rank tensor (Neumann's principle),[20] which is given by

$$\rho_{ij}' = l_{ip}l_{jq}\rho_{pq}. \quad \text{(B2)}$$

Using the last two Eqs. (B1) and (B2) the measured planar Hall resistivity in the (113) system, $\rho_{21}^{(113)}$, can now be derived

$$\rho_{21}^{(113)} = \frac{3}{2\sqrt{11}}(\rho_{21} + \rho_{22} - \rho_{11} - \rho_{12}) + \frac{1}{\sqrt{11}}(\rho_{13} - \rho_{23}). \quad \text{(B3)}$$

Since the demagnetization energy of these Fe$_3$Si films are rather large, the magnetization **M** is restricted to the (113) plane. In this case the direction cosines of **M** as used in our previous studies of Fe(113) films[19] can be shown to be $\alpha_1 = (3/\sqrt{22})\cos\theta_M - (1/\sqrt{2})\sin\theta_M$, $\alpha_2 = (3/\sqrt{22})\cos\theta_M + (1/\sqrt{2})\sin\theta_M$, $\alpha_3 = -(\sqrt{2/11})\cos\theta_M$, where θ_M is measured with respect to the $[33\bar{2}]$ axis. Using these direction cosines in Eqs. (A2), we can derive the measured planar Hall resistivity for the case of [113] oriented films in terms of θ_M

$$\rho_{21}^{(113)} = \frac{9C_1}{11}\cos\theta_M\sin\theta_M + \frac{81C_2}{121}\cos^3\theta_M\sin\theta_M$$

$$+ \frac{9C_2}{11}\cos\theta_M\sin^3\theta_M - \frac{18C_3}{121}\cos^3\theta_M\sin\theta_M$$

$$+ \frac{2C_4}{11}\cos\theta_M\sin\theta_M - \frac{9C_5}{121}\cos^3\theta_M\sin\theta_M$$

$$+ \frac{C_5}{11}\cos\theta_M\sin^3\theta_M + \frac{15(a_{12223} - a_{11123})}{121\sqrt{2}}\cos^3\theta_M$$

$$+ \frac{9(a_{12223} - a_{11123})}{11\sqrt{2}}\cos\theta_M\sin^2\theta_M. \quad \text{(B4)}$$

This equation is valid up to the fourth-order contribution of α_i and contains both symmetric and antisymmetric contributions. The symmetric part contains the coefficients C_i's. Note that terms containing the coefficients $C_2, C_3,$ and C_5 are fourth-order contributions of α_i [see Eq. (A2)]. Other symmetric terms containing the coefficients C_1 and C_4 are second-order contributions of α_i. The antisymmetric part which contains the tensor elements a_{12223} and a_{11123} are third-order contributions of α_i. Thus, if we consider terms up to third order in α_i we can write the above equation in the following form:

$$\rho_{21}^{(113)} = \frac{(9C_1 + 2C_4)}{22}\sin 2\theta_M + \frac{15(a_{12223} - a_{11123})}{121\sqrt{2}}\cos^3\theta_M$$
$$+ \frac{9(a_{12223} - a_{11123})}{11\sqrt{2}}\cos\theta_M\sin^2\theta_M, \qquad \text{(B5)}$$

which can also be expressed in the following form:

$$\rho_{21}^{(113)} = \frac{(9C_1 + 2C_4)}{22}\sin 2\theta_M + \frac{9(a_{12223} - a_{11123})}{11\sqrt{2}}\cos\theta_M$$
$$- \frac{42\sqrt{2}(a_{12223} - a_{11123})}{121}\cos^3\theta_M. \qquad \text{(B6)}$$

*Electronic address: muduli@pdi-berlin.de

[1] G. A. Prinz, Science **282**, 1660 (1998).

[2] S. A. Wolf, D. D. Awschalom, R. A. Buhrman, J. M. Daughton, S. von Molnár, M. L. Roukes, A. Y. Chtchelkanova, and D. M. Treger, Science **294**, 1488 (2001).

[3] J. D. Boeck, W. V. Roy, V. Motsnyi, Z. Liu, K. Dessein, and G. Borghs, Thin Solid Films **412**, 3 (2002).

[4] S. Fölsch, B.-C. Choi, and K. H. Rieder, Phys. Rev. B **54**, 10855 (1996).

[5] A. J. Freeman and R. Wu, J. Magn. Magn. Mater. **100**, 497 (1991).

[6] P. K. Muduli, J. Herfort, H.-P. Schönherr, and K. H. Ploog (to be published).

[7] J. Herfort, H.-P. Schönherr, and K. H. Ploog, Appl. Phys. Lett. **83**, 3912 (2003).

[8] D. A. Thompson, L. T. Romankiw, and A. F. Mayadas, IEEE Trans. Magn. **11**, 1039 (1975).

[9] T. McGuire and R. Potter, IEEE Trans. Magn. **11**, 1018 (1975).

[10] J. P. Jan, in *Solid State Physics*, edited by F. Seitz and D. Turnbull (Academic Press, New York, 1957), Vol. 5, pp. 1–96.

[11] This term was introduced by E. Gruneisen and J. Gielessen, Ann. Phys. **27**, 243 (1936).

[12] K.-J. Friedland, R. Nötzel, H.-P. Schönherr, A. Riedel, H. Kostial, and K. Ploog, Physica E (Amsterdam) **10**, 442 (2001).

[13] K. J. Friedland, J. Herfort, P. K. Muduli, H.-P. Schönherr, and K. H. Ploog, J. Supercond. (to be published).

[14] M. Hansen, *Constitution of Binary Alloys* (McGraw-Hill, New York, 1958).

[15] R. P. Elliot, *Constitution of Binary Alloys*, Suppl. 1 (McGraw-Hill, New York, 1965).

[16] The saturation field is rather low and is about 0.11 kOe, as is also evidenced from SQUID magnetometry.

[17] M. Bowen, K.-J. Friedland, J. Herfort, H.-P. Schönherr, and K. H. Ploog, Phys. Rev. B **71**, 172401 (2005).

[18] P. Granberg, P. Isberg, T. Baier, B. Hjörvarsson, and P. Nordblad, J. Magn. Magn. Mater. **195**, 1 (1999).

[19] P. K. Muduli, J. Herfort, H.-P. Schönherr, and K. H. Ploog, J.

Appl. Phys. **97**, 123904 (2005).

[20] R. R. Birss, *Symmetry and Magnetism* (North-Holland, Amsterdam, 1964).

[21] I. A. Campbell and A. Fert, in *Ferromagnetic Materials*, edited by E. P. Wohlfarth (North-Holland, Amsterdam, 1982), Vol. 3, p. 747.

[22] T. T. Chen and V. A. Marsocci, Solid State Commun. **10**, 783 (1972); Physica (Amsterdam) **59**, 498 (1972).

[23] J. F. Nye, *Physical Properties of Crystals: Their Representation by Tensors and Matrices* (Oxford University Press, London, 1985), p. 9, reprint ed.

[24] W. Döring, Ann. Phys. **32**, 259 (1938).

[25] E. Fawcett and W. A. Reed, Phys. Rev. Lett. **9**, 336 (1962).

[26] Y. C. Akgöz and G. A. Saunders, J. Phys. C **8**, 1387 (1975).

[27] B. Lenoir, F. Brochin, and J.-P. Michenaud, Europhys. Lett. **58**, 93 (2002).

[28] F. P. Beitel and J. E. M. Pugh, Phys. Rev. **112**, 1516 (1958).

[29] E. R. Sanford, A. C. Ehrlich, and E. M. Pugh, Phys. Rev. **123**, 1947 (1961).

[30] H. Ashworth, D. Sengupta, G. Schnakenberg, L. Shapiro, and L. Berger, Phys. Rev. **185**, 792 (1969).

[31] S. Foner, F. E. Allison, and E. M. Pugh, Phys. Rev. **109**, 1129 (1958).

[32] A. Sinha and A. K. Majumdar, J. Appl. Phys. **50**, 7533 (1979).

[33] B. Jenichen, V. M. Kaganer, J. Herfort, D. K. Satapathy, H.-P. Schönherr, W. Braun, and K. H. Ploog, Phys. Rev. B72, 075329 (2005).

[34] V. Niculescu, K. Raj, J. I. Budnick, T. J. Burch, W. A. Hines, and A. H. Menotti, Phys. Rev. B **14**, 4160 (1976).

[35] W. A. Hines, A. H. Menotti, J. I. Budnick, T. J. Burch, T. Litrenta, V. Niculescu, and K. Raj, Phys. Rev. B **13**, 4060 (1976).

[36] V. Niculescu, J. I. Budnick, W. A. Hines, K. Raj, S. Pickart, and S. Skalski, Phys. Rev. B **19**, 452 (1979).

[37] P. J. Webster and K. R. A. Ziebeck, in *Landolt-Börnstein-Group III Condensed Matter*, edited by P. J. Webster and K. R. A. Ziebeck (Springer-Verlag, Berlin, 1988), Vol. 19, pp. 75–79.